To be published in *ApJ Letter*

The ROSAT Deep Cluster Survey: the X-ray Luminosity Function out to $z = 0.8$

Piero Rosati,[1,2,3,4] Roberto Della Ceca,[5] Colin Norman,[2] and Riccardo Giacconi[1]

ABSTRACT

We present the X-ray Luminosity Function (XLF) of the ROSAT Deep Cluster Survey (RDCS) sample over the redshift range 0.05–0.8. Our results are derived from a complete flux-limited subsample of 70 galaxy clusters, representing the brightest half of the total sample, which have been spectroscopically identified down to the flux limit of 4×10^{-14} erg cm^{-2} s^{-1} (0.5–2.0 keV) and have been selected via a serendipitous search in ROSAT-PSPC pointed observations. The redshift baseline is large enough that evolutionary effects can be studied within the sample. The local XLF ($z \leq 0.25$) is found to be in excellent agreement with previous determinations using the ROSAT All-Sky Survey data. The XLF at higher redshifts, when combined with the deepest number counts constructed to date ($f > 2 \times 10^{-14}$ erg cm^{-2} s^{-1}), reveal no significant evolution at least out to $z = 0.8$, over a luminosity range $2 \times 10^{42} - 3 \times 10^{44}$ erg s^{-1} in the [0.5-2 keV] band. These findings extend the study of cluster evolution to the highest redshifts and the faintest fluxes probed so far in X-ray surveys. They complement and do not necessarily conflict with those of the Einstein Extended Medium Sensitivity Survey, leaving the possibility of negative evolution of the brightest end of the XLF at high redshifts.

Subject headings: galaxies: clusters: general — X-rays: general — cosmology: observations

[1]ESO - European Southern Observatory, D-85748 Garching b. München, Germany; prosati@eso.org

[2]Department of Physics & Astronomy, The Johns Hopkins University, Baltimore, MD, 21218

[3]Visiting Astronomer, Kitt Peak National Observatory. KPNO is operated by AURA, Inc. under contract to the National Science Foundation.

[4]Visiting Astronomer, Cerro Tololo Inter-American Observatory. CTIO is operated by AURA, Inc. under contract to the National Science Foundation.

[5]Osservatorio Astronomico di Brera, 20121 Milano, Italy

1. Introduction

Large homogeneous samples of galaxy clusters, spanning a wide range of redshifts, have long been considered powerful tools to study the evolution of the large scale structures in the Universe. Unfortunately, finding clusters at cosmologically interesting lookback times, i.e. $z > 0.5$, not to mention defining a complete sample, is a time consuming and difficult task. As a result, the much-needed observational constraints for theories of cluster formation have not been forthcoming.

In an effort to remedy this situation, we have embarked on a project, the ROSAT Deep Cluster Survey (RDCS), aimed at constructing a large homogeneous sample of distant galaxy clusters selected solely on the basis of their X-ray properties from ROSAT-PSPC pointed observations. Initial results have been presented in Rosati et al. 1995 (R95). Pure X-ray selection leads to a selection function which can be modelled in a relatively straightforward way, being essentially that of a flux limited sample. As a result, distribution functions of observables, such as the number counts, the X-ray Luminosity Function (XLF) and the redshift distribution, can be directly compared with theories of structure formation. Until very recently, the only available sample of X-ray selected clusters at high redshifts was the one compiled from the Einstein Extended Medium Sensitivity Survey (EMSS) (Gioia et al. 1990, Henry et al. 1992 (H92)). From a complete subsample of 67 clusters at $0.14 < z < 0.6$, the authors found evidence of a statistically significant negative evolution of the XLF at $z \gtrsim 0.3$ and $L_{X[0.3-3.5]\ \mathrm{keV}} \gtrsim 5 \times 10^{44}$ erg s^{-1}. Earlier claims of strong evolution at lower redshifts (Edge et al. 1990) have been ruled out by a large compilation of X-ray clusters from the ROSAT All-Sky Survey (RASS) (Ebeling et al. 1997). More recently, the EMSS findings have been challenged by a re-analysis of the same sample supplemented by ROSAT data (Nichol et al. 1997). Covering a very large solid angle (735 deg^2), but being relatively shallow, the EMSS sample can probe mostly the bright end of the XLF and can provide weak constraints on the evolution of the XLF at higher redshifts since only 6 EMSS clusters lie at $z > 0.5$. On the other hand, the RDCS reaches considerably fainter fluxes, but covers a much smaller solid angle and therefore probes a complementary region in the $L_X - z$ plane to the EMSS. Surveys similar to the RDCS, utilizing the PSPC archival data and somewhat different selection techniques, are now well underway (RIXOS (Castander et al. 1995), SHARC (Collins et al. 1997, Burke et al. 1997), WARPS (Scharf et al. 1997)).

In this Letter, we present the XLF constructed from a flux-limited, spectroscopically confirmed subsample of the RDCS. This subsample is already as large as the EMSS sample and covers a wider redshift range, from the local universe (z=0.05) out to $z \simeq 0.8$. Therefore, we can compare our low-redshift luminosity function with recent determinations from cluster samples compiled from the ROSAT All-Sky Survey (Burns et al. 1996, Ebeling et al. 1997). Furthermore, we can compare, for the first time, the space density of high redshift clusters with the findings of the EMSS and extend the study of cluster evolution to even higher redshifts. We adopt $H_0 = 50$ km s^{-1} Mpc^{-1} and $q_0 = 0.5$ througout.

2. The Cluster Sample

A full discussion of the analysis of the X-ray data and the selection technique for the RDCS sample is presented in R95. Cluster candidates are selected from a serendipitous search for extended X-ray sources in deep pointed observations drawn from the ROSAT-PSPC archive. A wavelet-based technique, which is particularly efficient at reducing the effects of confusion and is not biased against low surface brightness features, is used to detect and characterize X-ray sources. A control sample of about 5000 point sources is used to establish the mean and the variance of the PSF at different off-axis angles (θ), thereby assessing the statistical significance for a source to be extended. Cluster candidates are selected as those sources extended at 99% confidence level and having a flux $f_{-14} = f_X[0.5-2.0]\mathrm{keV}/(10^{-14}$ erg cm^{-2} s$^{-1}) > 1$ and $\theta < 18$ arcmin. This selection technique yielded 160 cluster candidates over an area of about 48 deg^2, drawn from 170 X-ray fields scattered across the two galactic caps ($|b| > 20^\circ$).

The completeness flux limit of the survey is determined by the flux level at which extended and point-like emission can be reliably distinguished. In addition to the source flux, this critically depends on the off-axis angle θ within which the candidates are selected, due to PSF degradation. From a consideration of surface brightness dimming alone, one expects the fraction of clusters which are unresolved by the PSPC at high redshifts to increase at faint flux levels and at high off-axis angles. These effects are analyzed in detail elsewhere (Rosati & Della Ceca, in preparation). The selection function is modelled and quantified using a combination of simulations, control samples of known distant clusters and by studying cluster number counts as a function of (f_X, θ). This analysis allows two statistically complete and independent samples to be defined: one deeper (Sample A), covering $\sim$33 deg^2 ($f_{-14} > 1, \theta \leq 15'$) and one shallower (Sample B) with $f_{-14} > 6$ and $15' < \theta \leq 18'$. By combining these distinct samples the surveyed area increases to $\sim$48 deg^2. We have chosen a higher flux limit for Sample B since it becomes significantly incomplete for $f_{-14} < 5$. The incompleteness of Sample A is measured to be negligible for $f_{-14} > 4$, is about 10% at $f_{-14} \simeq 2$ and drops to $\sim 20-25\%$ at $1 < f_{-14} < 2$.

The sky coverage Ω of the survey, as emphasized in R95, also depends on the intrinsic angular size (Θ) of the source for a given flux, i.e. $\Omega = \Omega(f, \Theta)$. Here, for the sake of simplicity, we have reduced this bivariate function to a function of the flux only, by choosing a value $\bar{\Theta}$ equal to the median angular size of the clusters in the whole sample after deconvolving the PSF ($\bar{\Theta} \simeq 58''$). We have verified that the use of this effective sky coverage is equivalent to the general method described in R95. The function $\Omega = \Omega(f, \bar{\Theta})$ for Sample A and its extension $(A + B)$ is shown in fig.1.

3. Optical Follow-up Observations

In order to identify these cluster candidates, we have undertaken a large optical follow-up program, consisting of deep imaging using the KPNO 4m and 2.1m and the CTIO 4m and

1.5m, and multislit spectroscopy carried out with KPNO 4m and the ESO 3.6m. The imaging survey in V and I bands is now 90% complete and has revealed a very high success rate of identification, with about 115 new clusters (or groups) confirmed to date, i.e. displaying a significant overdensity of galaxies around the peak of the X-ray emission. More importantly, the spectroscopic follow-up work has secured 95 cluster redshifts so far, spanning the range 0.045–0.83. Most of the spectroscopic identifications are based on more than 3 redshifts within 1500 km/s, with a median value of 5 members per cluster. A significant fraction of the newly discovered clusters lie at high redshift, about one-third at $z > 0.4$ and a quarter at $z > 0.5$, making the RDCS the largest sample of spectroscopically confirmed distant clusters compiled to date. Details on the optical observations of the whole RDCS catalogue will be published elsewhere.

4. The X-ray Luminosity Function

The imaging and spectroscopic identification of the cluster candidates in Sample A is 97% complete down to $f_{-14} = 4$, hence a complete flux limited subsample of 70 clusters with measured redshifts can be defined[6]. We split the sample in three redshift shells, [0.045–0.25], [0.25–0.5], [0.5-0.85], where we have respectively 33, 23, 14 clusters. The luminosities in the observed [0.5–2.0] keV band range from 3.5×10^{44} to 1×10^{42} erg s^{-1} and thus probe the region of moderately rich clusters to poor groups. A non-parametric representation of the XLF has been obtained using the $1/V_a$ method of Avni and Bahcall (1980). The application of this procedure for deriving the XLF in different redshift shells is fully described in Maccacaro et al., 1991. For each luminosity bin containing n objects, the differential XLF is computed as, $dN(L)/dL = \sum_{i=1}^{n} 1/(V_{S_i} \Delta L)$, where V_{S_i} represents the total search volume for object i and ΔL is the width of the luminosity bin. Bins of equal logarithmic width $\Delta Log\ L = 0.3$ have been used. The corresponding 68% error bars have been determined using Poissonian statistics (following Wolter et al. 1994). A power law spectrum with energy index 0.5, which well approximates a Raymond-Smith spectrum over a large temperature range in the [0.5-2.0] keV band, has been used for computing k-corrections. Count rates have been converted to fluxes according to R95.

The XLF derived is shown in fig.2. We point out the excellent agreement between the local XLF of the RDCS, i.e. in the lowest redshift bin, and two independent determinations of the local XLF from Ebeling et al. 1997 and Burns et al. 1996 (B96). Both these surveys use RASS data but completely different selection techniques. The Bright Cluster Sample (BCS) of Ebeling et al. 1997 is an X-ray flux limited sample out to $z = 0.3$ thus covering the intermediate and bright end of the XLF, whereas the B96 sample is an optically selected, volume complete, sample of nearby groups and poor clusters ($z \leq 0.15$) which probes mostly the faint end, down to luminosities well

[6] To date, only two candidates have not been identified down to the flux limit of $f_{-14} = 4$. These are extended X-ray sources which may be either a blend of multiple sources, for which we did not find an obvious optical counterpart, or high redshift clusters, for which deeper imaging is required.

below 10^{42} erg s^{-1}. The RDCS XLF in the first redshift shell is well fit by a power law in the form $n(L_{44}) = KL_{44}^{-\alpha}$, where L_{44} is the X-ray luminosity in the the rest frame band [0.5-2.0]keV in units of 10^{44} erg s^{-1} and K is in units of 10^{-7}Mpc$^{-3}[L_{44}]^{(\alpha-1)}$. A maximum-likelihood fit yields: $\alpha = 1.83 \pm 0.15$ and $K = 3.26 \pm 0.57$. These parameters compare favorably with those of B96, $\alpha = 1.71 \pm 0.19$ and $K = 3.50 \pm 0.77$ (after rescaling to $H_0 = 50$ km s^{-1} Mpc^{-1}), and the power law part of the Schechter XLF of the BCS sample, $\alpha = 1.85 \pm 0.09$ and $K = 3.32(^{+0.36}_{-0.33})$. A different cluster sample, analogous to the BCS, compiled from the RASS in southern sky provides similar results (De Grandi, 1996). The excellent agreement found between these independent determinations is by no means trivial since the RDCS is the only sample of the four whose selection *is not driven by any optical information*, but purely by the X-ray properties of clusters. Indeed, it suggests that systematic effects in local cluster samples seem to be now well under control.

The inspection of the RDCS XLF in the higher redshift bins does not show any significant evolution, at least out to $z \simeq 0.8$, over the probed luminosity range. Based on the number of high redshift clusters in the SHARC-South sample Collins et al. 1997 also found no evidence of significant negative evolution. More recently, Burke et al. 1997 have contructed the XLF from the same small SHARC-S sample, 16 clusters in the range $0.3 < z < 0.7$, and have reached similar conclusions to the ones reported in this work. The large fraction of high redshift clusters in the RDCS cannot be reconciled with the results of the RIXOS survey (Castander et al. 1995). A factor of 4 more RDCS clusters have been identified at $z > 0.4$ compared to the RIXOS survey down to the same flux limit ($f_{-14} = 3$) and over the same solid angle. This difference may partly be due to incompleteness or small number statistics in RIXOS, but also may reflect an overestimate of the sky coverage of the RIXOS survey at low fluxes ($\Omega(f, \Theta)$ is assumed constant) which could mimic a dearth of clusters at high redshifts (Rosati & Della Ceca, 1996).

Given its relatively small surveyed area, the RDCS cannot probe the XLF *above* $L_X \simeq 3 \times 10^{44}$ erg s^{-1}. This is the luminosity range where the EMSS sample finds evidence of negative evolution, i.e. a steepening of the high end of the XLF at $z \gtrsim 0.3$ (Gioia et al. 1990). A direct comparison of the cluster volume densities of the RDCS and EMSS samples is illustrated in fig.3, where we recompute the XLF of the RDCS sample in the redshift shell [0.3–0.6] (24 objects), the highest redshift shell of the EMSS sample. The XLF data points of the EMSS sample (open and filled squares) have been converted to the 0.5–2.0 keV band by recomputing the XLF using the sample, the sky coverage and the method of H92, updating a few redshifts and identifications according to Gioia & Luppino 1994. A power law spectral model with energy index 0.5 has been used to convert fluxes from 0.3–3.5 to 0.5–2.0 keV band. We have verified that the same XLF data points of H92 are obtained within 10% in the original 0.3–3.5 keV band. We note the excellent agreement between the RDCS and the EMSS samples in the lowest redshift bin, where the respective XLFs overlap. More importantly, the EMSS XLF in the high redshift shell is consistent within the errors with the RDCS XLF over the luminosity range $8 \times 10^{43} - 3 \times 10^{44}$. The RDCS however, cannot follow the drop of the EMSS at the bright end of the XLF.

5. Cluster Number Counts

In addition to the spectroscopically confirmed sample, a larger number of cluster candidates have been identified from imaging data. We can now compute the cluster number counts from a sample of 130 candidates drawn from Sample A+B down $f_{-14} = 2$, 90% of which have positive identification. We do not attempt here to extend this analysis below $f_{-14} = 2$ since the optical identification is still largely incomplete at such low fluxes. The resulting cluster $\log N$–$\log S$, which significantly improves the one of R95, is shown in fig.4 along with previous determinations. The error bars take into account the statistical uncertainties as discussed in R95 and the systematics due to flux measurements. The latter typically increase the upper error bar of $N(>S)$ by +15% at high fluxes as a result of the possible lost flux in the evaluation of the wavelet algorithm. The faintest three data points have been corrected for the small 10% incompleteness. These surface densities are in good agreement with those of the WARPS survey (Jones et al., 1997) above their flux limit $f_{-14} = 6$. A maximum likelihood fit to the differential number counts with a double power law model, $K_1 S^{-\alpha_1}$ for $s \geq S_B$, $K_1 S_B^{(\alpha_2-\alpha_1)} S^{-\alpha_2}$ for $s \leq S_B$, yields: $\alpha_1 = 2.22 \pm 0.15$, $\alpha_2 = 1.91 \pm 0.18$, $S_B = 1.03 \pm 0.05$, $K_1 = 1.10 \pm 0.15$ deg^{-2}, where fluxes are in units of 10^{-13} erg cm^{-2} s^{-1}. This curve can be integrated to provide the cluster contribution to the soft X-ray background, $I_{CXB}(0.5-2\,\mathrm{keV}) \simeq 1.5\,\mathrm{keV\,cm^{-2}s^{-1}sr^{-1}}$ down to $f_{-14} = 1$, and is found to account for about 10% of the observed soft extragalactic X-ray background.

Given the accurate determination of the local XLF (fig.2), which we parametrize as the BCS Schechter XLF with the RDCS faint slope, we can now compare our cluster $\log N$–$\log S$ with the predicted number counts for a non-evolving XLF. In fig.4 we show that these predictions, obtained by integrating the local XLF over the probed redshift and luminosity range for two values of q_0, are very close to the observed counts. We note that these number counts are drawn from a sample which is a factor 2 deeper than the one used to compute the XLF. The $\log N$–$\log S$ at low fluxes is very sensitive to the faint end slope of the XLF, as well as its evolution, which is not directly probed by the RDCS XLF in the two highest redshift bins. A significant steepening (or flattening) ($|\Delta\alpha| > 0.2$) of the faint end ($L_X < 10^{43}$ erg s^{-1}) of the XLF at $z > 0.3$ would lead to an overprediction (or underprediction) of the observed faint number counts outside the error bars, for any value of $0 \leq q_0 \leq 0.5$. This further strengthens the evidence that the XLF does not evolve, within the present uncertainties, over a wide range of luminosities ($2 \times 10^{42} \lesssim L_X(\text{ erg s}^{-1}) \lesssim 3 \times 10^{44}$). The implications that these faint number counts have for CDM models of cluster formation have been explored by Kitayama & Suto (1997) and Mathiesen & Evrard (1997).

6. Conclusions

The large size of the RDCS sample and its wide redshift baseline allow us to provide an accurate assessment of the evolution of the space density of galaxy clusters over a considerable

range in X-ray luminosities and out to the highest redshifts probed so far in X-ray surveys. We find an excellent agreement with independent determinations of the local XLF. By combining the RDCS XLF with an improved determination of faint cluster number counts, we find that the XLF does not evolve significantly at $z \lesssim 0.8$ in the luminosity range ($2 \times 10^{42} - 3 \times 10^{44}$ erg s^{-1}). Our results extend and complement those of the EMSS, further restricting the possibility of negative evolution in the X-ray cluster population at $z \gtrsim 0.3$ to only those clusters with X-ray luminosities in excess of the local $L^*_{[0.5-2]\mathrm{keV}} \simeq 4 \times 10^{44}$ erg s^{-1}.

We thank the TACs of Kitt Peak National Observatoty, Cerro Tololo Inter-American Observatory and the European Southern Observatory for the allocation of generous observing time and the staff of all the observatories for their excellent support. PR acknowledges support from NASA ADP grant NAG 5–3537.

REFERENCES

Burke, D.J., Collins, C.A., Sharples, R.M., Romer, A.K., Holden, B.P., Nicol, R.C. 1997 ApJ, in press

Burns, J.O. et al. 1996, ApJ, 467, L49

Castander, F.J. et al. 1995, Nature, 377, 39

Collins, C.A., Burke, D.J., Romer, A.K., Sharples, R.M., Nichol, R.C. 1997, ApJ, 479, L117

De Grandi, S. 1996, in MPE Report 263, Proceedings of Röntgenstrahlung from the Universe, ed. Zimmermann H.U., Trümper, J., Yorke, H. (Munich:MPE), 577

Ebeling H., Edge, A.C, Fabian, A.C., Allen, S.W., Crawford, C.S., Böhringer, H. 1997, ApJ, 479, L101

Edge, A.C., Stewart, G.C., Fabian, A.C, Arnaud, K.A. 1990, MNRAS, 245, 559

Gioia, I.M., Henry, J.P., Maccacaro, T., Morris, S.L., Stocke, J.T., Wolter, A. 1990, ApJ, 356, L35

Gioia I.M. & Luppino, G.A. 1994, ApJS, 94, 583

Henry, J.P., Gioia, I.M., Maccacaro, T., Morris, S.L., Stocke, J.T., Wolter, A. 1992, ApJ, 386, 408 (H92)

Jones, L.R., Scharf, C.A., Ebeling, H., Perlman, E., Wegner, G., Malkan, M., Horner, D. 1997, ApJ, in press

Kitayama, T. & Suto, S. 1997, ApJ, in press

Maccacaro, T., Della Ceca, R., Gioia, I.M., Morris, S.L., Stocke, J.T., Wolter, A. 1991, ApJ, 374, 117

Mathiesen, B. & Evrard, A.E. 1997, MNRAS, in press

Nichol, R.C., Holden, B.P., Romer, A.K., Ulmer, M.P., Burke, D.J., Collins, C.A. 1997, ApJ, 481, 644

Rosati, P. & Della Ceca, R. 1996, in MPE Report 263, Proceedings of Röntgenstrahlung from the Universe, ed. Zimmermann H.U., Trümper, J., Yorke, H. (Munich:MPE), 613

Rosati, P., Della Ceca, R., Burg, R., Norman, C., Giacconi, R. 1995, ApJ, 445, L11 (R95)

Scharf, C.A., Jones, L.R., Ebeling H., Perlman, E., Malkan, M., Wegner, G. 1997, ApJ, 477, 79

Wolter, A., Caccianiga, A., Della Ceca R., Maccacaro, T. 1994, ApJ, 433, 29

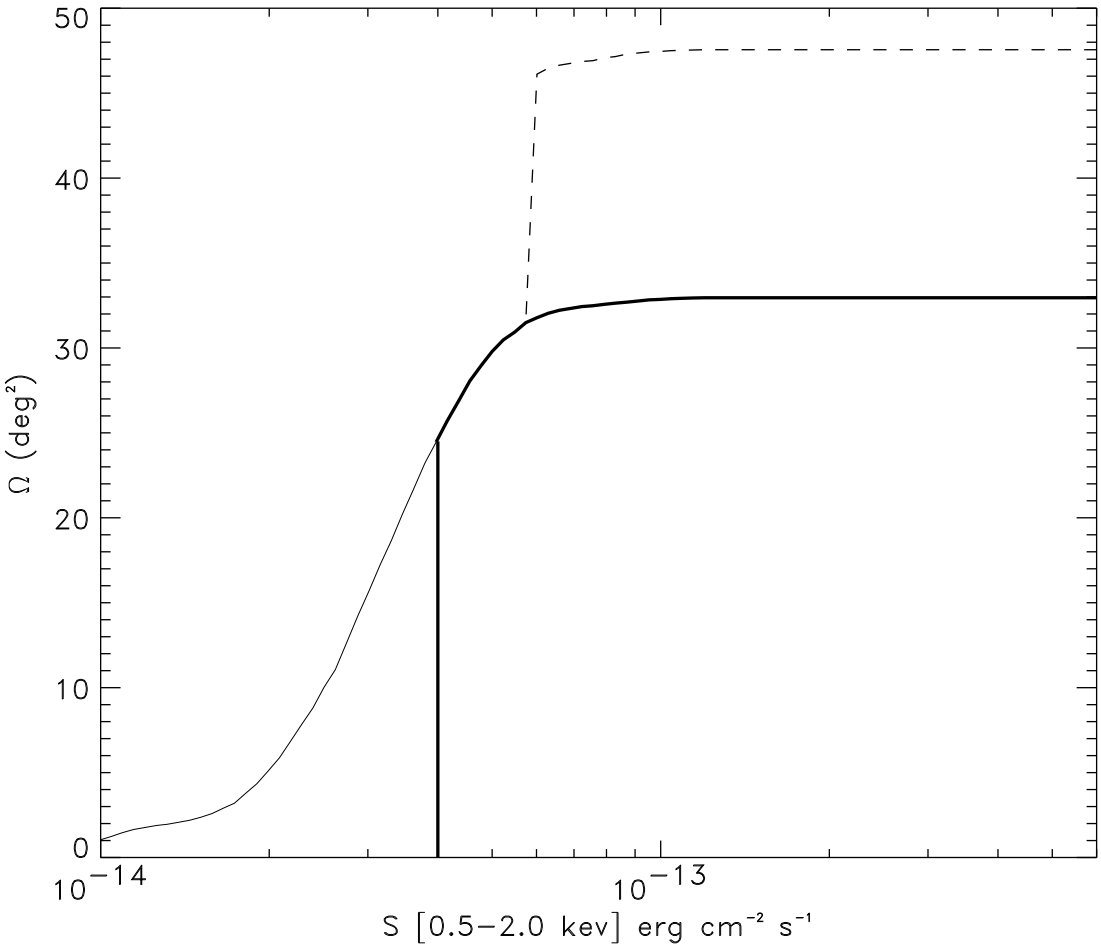

Fig. 1.— The effective sky coverage of the RDCS for Sample A (solid line) and its extension, Sample A + Sample B (dashed line). The thick solid line denotes the spectroscopically confirmed subsample used for computing the XLF.

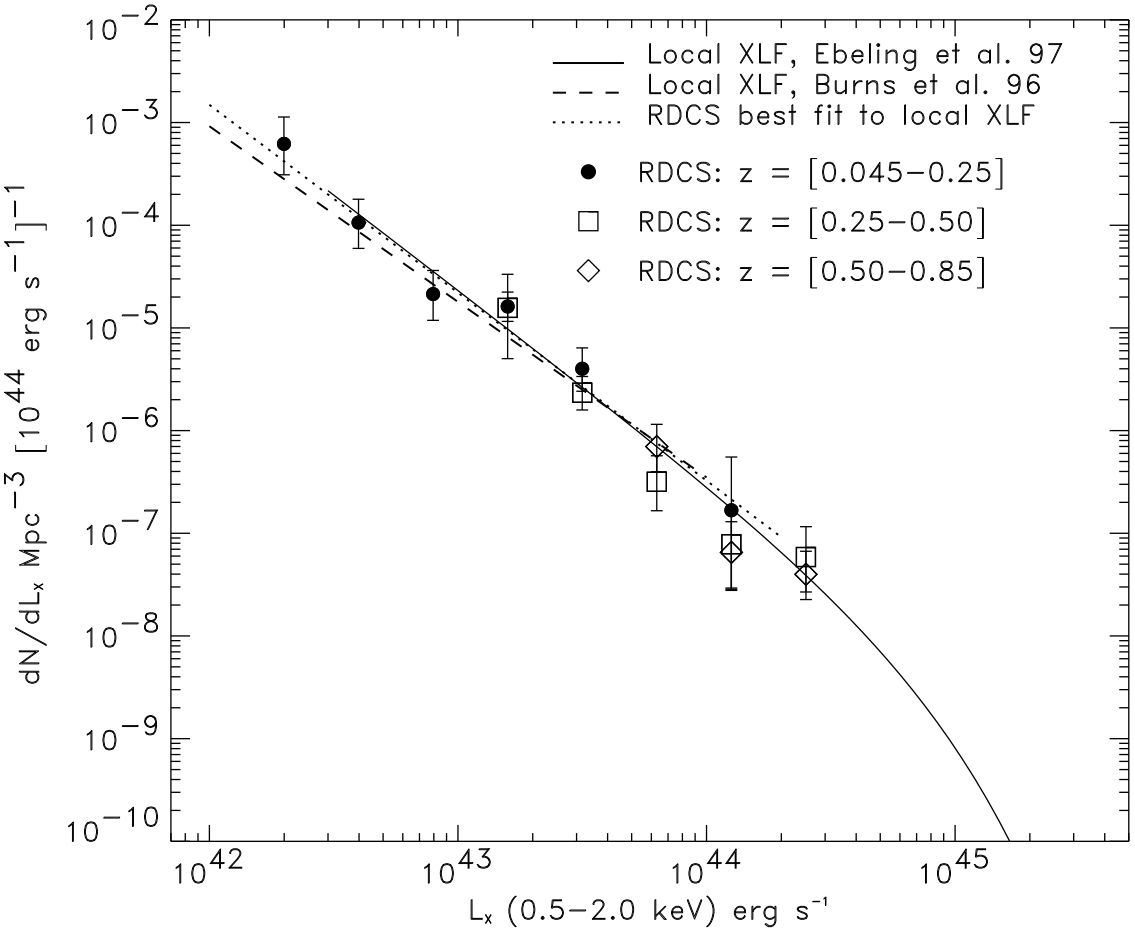

Fig. 2.— The X-ray cluster luminosity function for the RDCS sample in three redshift shells. Independent determinations of the local XLF from ROSAT All-Sky Survey data are also shown (dashed and solid lines).

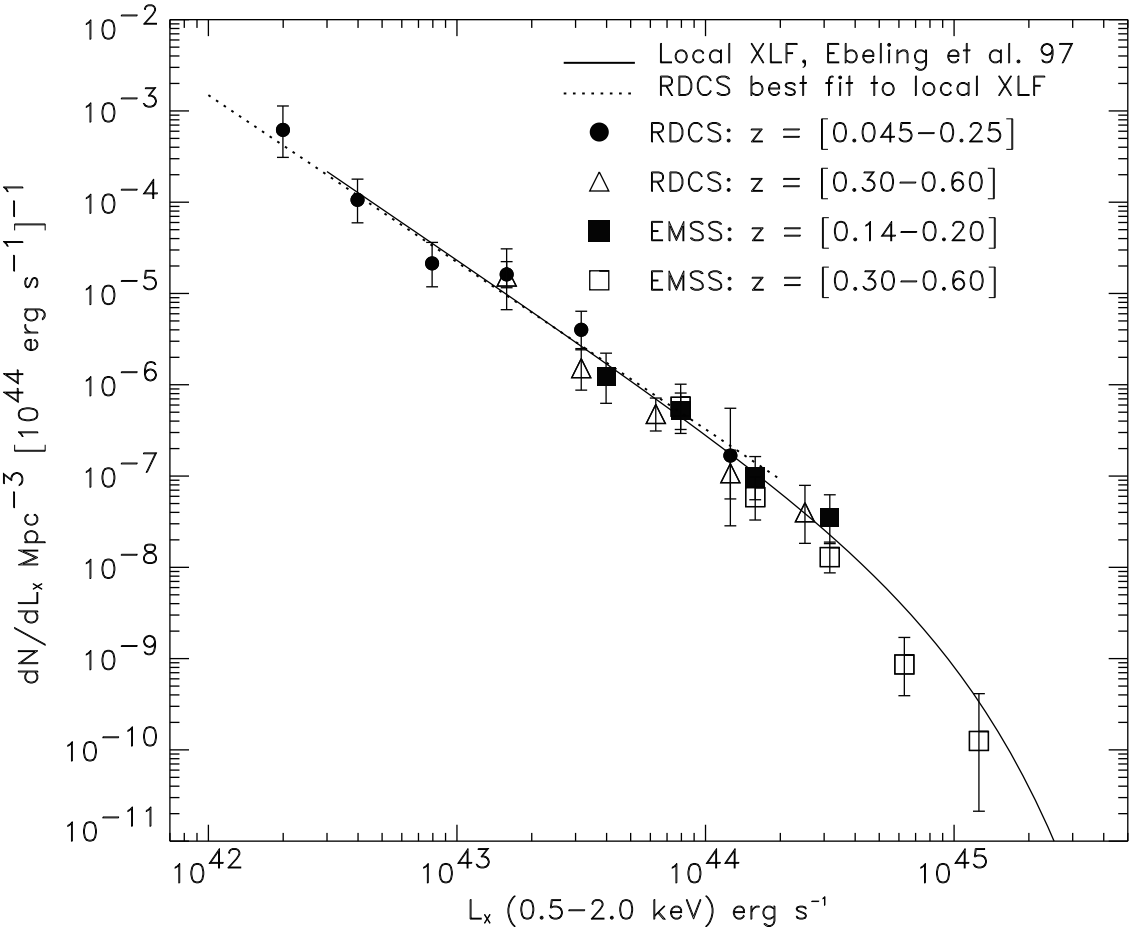

Fig. 3.— Comparison of the luminosty functions for the RDCS and the EMSS samples at low and high redshifts.

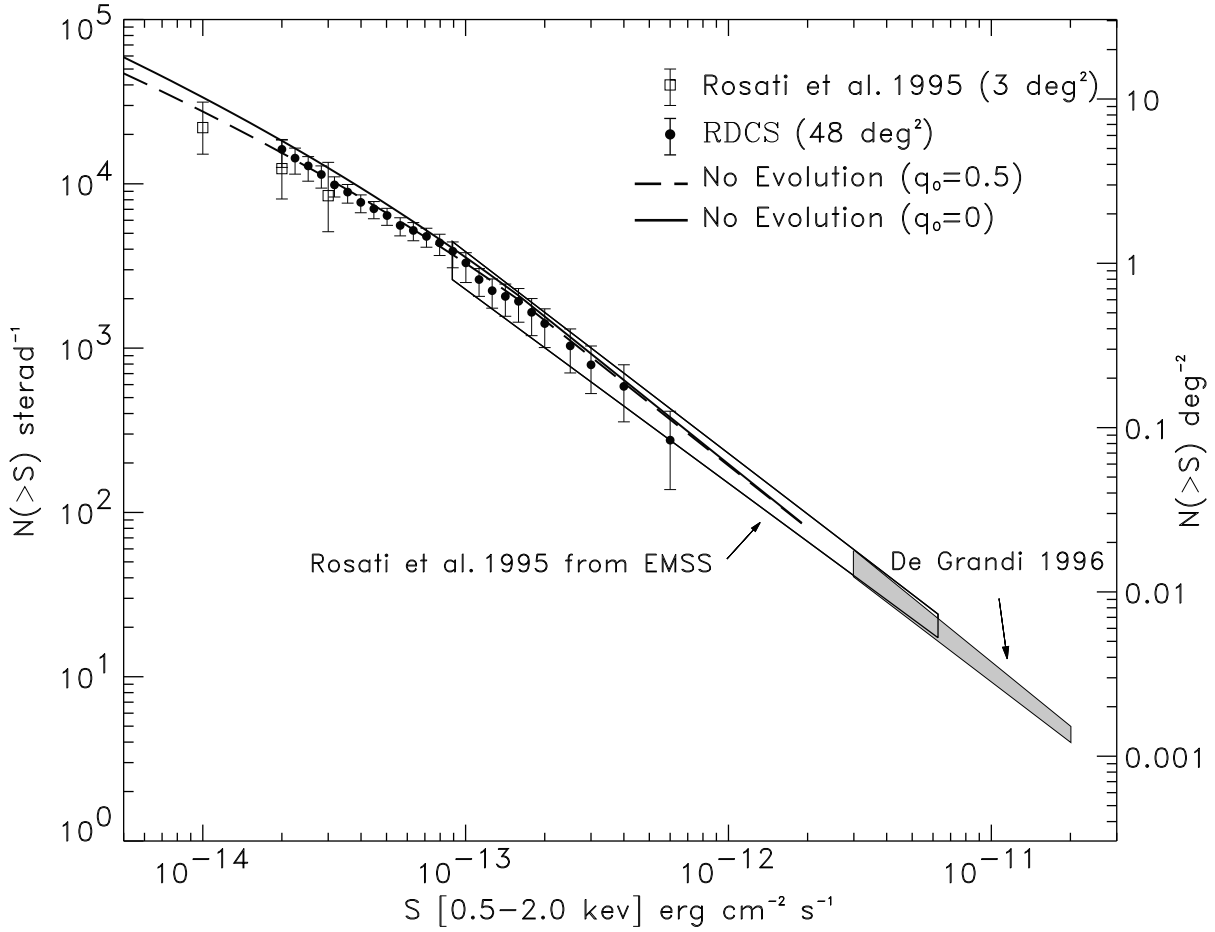

Fig. 4.— Observed cluster cumulative number counts for the RDCS sample (Sample A + B) and previous determinations. The no evolution curves were computed by integrating the best determination of the local XLF (see text) over the luminosity range $1 \times 10^{42} - 5 \times 10^{45}$ erg s^{-1} out to $z = 1.1$.